Studies on the Kinetics of Orientation and Crystallization of Nylon-66 During High-Speed Melt Spinning

HUAPING WANG, BIAO WANG, XUECHAO HU

College of Materials Science and Engineering, Donghua University, Shanghai, 200051 China

Received 11 July 2000; revised 10 November 2000; accepted 28 November 2000

ABSTRACT: A new way of applying on-line experimental data and basic theory to study the mechanism of orientation of a high-speed melt spinning process is described. The relationship of birefringence and stress for Nylon-66 was developed to understand the phenomena in the spinning line. The value of birefringence along the spinning line was calculated by various models to predict the orientation change. By comparison of the model prediction and on-line experimental birefringence, a suitable mechanical model to simulate the change of the profiles along the spinning line was chosen, and the structural development mechanism is discussed. The results show that the orientation mechanism of high-speed melt spinning of Nylon-66 is determined by deformation and deformation rate along the spinning line. For Nylon-66, molecular and crystal orientations develop independently and are controlled by the rotation of crystals and chain segments in the deformation field. © 2001 John Wiley & Sons, Inc. J Appl Polym Sci 82: 3157–3163, 2001

Key words: high-speed spinning; Nylon-66; orientation mechanism

INTRODUCTION

High-speed melt-spinning technology provides big industrial benefits, such as increased productivity, simplification of the process, reduction of energy, labor, and total production costs, etc., so examination of the fundamentals of the high-speed spinning process has drawn much attention from researchers. There have been a number of attempts to mathematically model the melt-spinning process,[1–6] but most have omitted crystallization phenomena because of the difficulties of treating nonisothermal crystallization and the effects of molecular orientation. The omission of crystallization phenomena from the model has made it impossible to understand how the final structure and properties of melt-spun filaments are developed. This information is particularly important for high-speed melt spinning of polymers, like PET, Nylon-66, etc.

An overall picture of the extent of understanding of the various physical processes and mathematical model of high-speed melt spinning is contained in the book by Ziabicki.[7] Katayama and Yoon[8] and Shimizu et al.[9] have developed models that include the effect of crystallization and applied these models to the melt spinning of PET. Zieminski and Spruiell[10] developed a mathematical model that was similar to that described by Shimizu et al., and applied it to the simulation of the high-speed melt spinning of Nylon-66. Because this model included the effects of acceleration, air drag, and gravity on the process dynamics and the effects of temperature and amorphous molecular orientation on the crystallization on kinetics, many researchers have quoted this model to simulate various high-speed melt-spinning processes and have applied it to the study of

Correspondence to: B. Wang (wbiao2000@citiz.net).

Journal of Applied Polymer Science, Vol. 82, 3157–3163 (2001)

the structural developmental mechanism. The model could partly explain many phenomena at the spinning line, like that of the temperature, diameter, and velocity profiles, but there is still much disagreement between predicted profiles and the on-line experimental results, such as birefringence profile, etc. However, to date, there is no systematic mechanism to account for orientation and orientation-induced crystallization along the spinning path, primarily because the distribution of orientation and stress at the spinning line is changing with increasing crystallization and polymers with various orientation structure are not available. Until now, only diameter, temperature, and birefringence on-line measurement profiles have been available. Many off-line results can not help accurately explain the structural development mechanism. Even with the incorporation of orientation distributions, there still remains the question of how to describe the temperature and orientation effects on the crystallization kinetics. The formulation used in the earlier model is a result of empiricism and a simplified theoretical development by Ziabicki.[7] This simplified development is due in part to the large difficulties associated with designing an experiment to actually study the crystallization kinetics of an oriented material, maintaining and completely characterizing the orientation during crystallization, and the lack of a fundamental theoretical basis for the nucleation and growth phases of the crystallization process in oriented polymers.

Applying the limited on-line experimental data and some basic theory to study the mechanism of orientation and crystallization of high-speed melt-spinning process is a new way to understand the phenomena happened in the spinning line. In this paper, with the help of some basic relationships described by Zieminski, Sprueill, and Shimizu et al.,[1–10] we apply the existing the on-line experimental data to study the main factors that affect the orientation and verify the relationship between the birefringence and deformation and deformation rate developed by Zieminski and Sprueill.[10] The dynamic mechanism of orientation is also discussed.

FUNDAMENTAL EQUATION

The fundamental equations are developed from the equations of continuity, momentum, and energy by applying the kinematics of melt spinning and the following assumptions:

(1) steady state;
(2) no radial variation;
(3) the tangential and radial velocities are zero;
(4) the surface tension of the polymer air interface, F_s, is negligible;
(5) viscous heating is negligible; and
(6) conduction and radiation are negligible.

These assumptions lead to the following set of working relationships:

$$\text{Continuity Equation: } G = \rho \frac{\pi D^2}{4} V \tag{1}$$

$$\text{Momentum Balance Equation: } \frac{dF}{dx} = G\frac{dV}{dx} + \frac{1}{2} C_d V^2 \pi D \rho - \frac{Gg}{V} \tag{2}$$

$$\text{Energy Balance Equation: } \frac{dT}{dx} = \frac{h\pi D(T_s - T)}{GC_p} + \frac{\Delta H}{C_p}\frac{d\theta}{dx} \tag{3}$$

$$\text{Constitutive Equation: } \frac{dV}{dx} = \frac{F\rho V}{G\eta} \tag{4}$$

where D, V, F, T, and θ are filament diameter, axial velocity, spinning line tension, filament temperature, and crystallinity, respectively, at a distance x from the spinneret; ρ, C_{op}, ΔH, and C_p are density, stress optical coefficient, heat of fusion, and specific heat of Nylon-66, respectively; C_d and h are air drag coefficient and convective coefficient, respectively; G and g are mass throughput and acceleration of gravity, respectively; ρ_a and T_s are air density and cooling air temperature, respectively; and η is elongational viscosity. More details are given elsewhere.[10]

To apply the relationships just presented to the melt-spinning process, expressions for the drag coefficient, heat transfer coefficient, molecular orientation, and crystallization kinetics are needed. The drag coefficient is derived by Sakiadis[11] from boundary layer theory as

$$C_d = aN_{\text{Re}}^b \tag{5}$$

where Re is the Reynolds number, and a and b are 0.507 and -0.61, respectively.

Table I Values of Important Physical Parameters Used in Numerical Solutions[a]

C_{op}	Δa^0	Δc^0	ΔH	θ_∞	θ_0	T_{max}	D_0	T_m
1.3×10^{-10} cm^2/dyne	0.090	0.090	45 cal/g	45%	0	150°C	80°C	225°C

[a] T_{max}, T_m, θ_∞, and C_{op} are temperature at maximum crystallization rate, equilibrium melting temperature, ultimate crystalline index, and stress optical coefficient, respectively.

The heat transfer coefficient with transverse flow of cooling air is computed with empirical relationship of Kase and Matsuo[4]:

$$h = 0.437 \times 10^{-4} A^{-0.334} V_y^{0.334} \left[1 + \left(\frac{8V}{V_y} \right)^2 \right]^{0.167} \quad (6)$$

A number of relationships were needed to describe the physical properties of Nylon-66 as a function of temperature, molecular weight, crystallinity, etc. The rheology of Nylon-66 is modeled as a Newtonian material

$$\sigma = \eta \frac{dV}{dx} \quad (7)$$

where the elongation viscosity is temperature, molecular weight, and crystallinity dependent. At temperatures above the xxxx (T_m), an Arrhenius expression was used to describe the temperature dependence

$$\eta = 3.31 \times 10^{-17} (M_n)^{3.5} \exp\left[\frac{7548}{T + 273} \right] \exp\left[4.605 \left(\frac{\theta}{\theta_\infty} \right)^2 \right] \quad (8)$$

In contrast, at temperatures $< T_m$, a WLF expression is used

$$\eta = 1.1 \times 10^{-11} (M_n)^{3.5} \exp\left[\frac{-8.86(T - 100)}{T + 1.6} \right] \times \exp\left[4.605 \left(\frac{\theta}{\theta_\infty} \right)^2 \right] \quad (9)$$

The density of Nylon-66 is given by[12]

$$\rho = [4.86 \times 10^{-4} T + 0.891]^{-1} \qquad (T \geq T_m) \quad (10)$$

$$\rho = \frac{1.1018 - 0.00151\theta}{1 - 0.128\theta} - 4.55 \times 10^{-4} T \qquad (T < T_m) \quad (11)$$

The specific heat was calculated as follows[13]:

$$C_p = 1.4 \times 10^{-3} T + 0.33 \quad (12)$$

The amorphous orientation and the birefringence along the spinning line are calculated by eqs. 13 and 14, respectively:

$$f_a = \frac{\Delta n_a}{\Delta a^0} \quad (13)$$

$$\Delta n = \theta \times f_c \times \Delta_c^0 + (1 - \theta) \times \Delta n_a \quad (14)$$

where Δn, Δn_a, f_a, Δ_a^0, Δ_c^0, f_c are birefringence, amorphous birefringence, amorphous orientation factor, amorphous intrinsic birefringence, crystalline intrinsic birefringence, and crystalline orientation factor, respectively.

The values of important physical parameters used in numerical solutions are given in Table I.[14–16] The conditions for the high-speed melt spinning of Nylon-66 are shown in Table II.

NUMERICAL SOLUTIONS

The Nylon-66 used in this investigation was supplied by Monsanto Textile and Intermediates Company. The number-average molecular weights (M_n) were computed using the Mark-Houwink coefficients of Taylor.[17] The filaments were melt spun from a Fourne Associates screw extruder with a 13-mm diameter screw. The polymer was metered through a gear pump to a single-hole spinneret with a capillary diameter of 0.635 mm and a length-to-diameter ratio of 6. The mass throughput was maintained constant at 2.5 g/min, and the extrusion temperature was 275 °C. The draw down device was placed 2.5 m below the spinneret. On-line measurements of diameter D_i, temperature T_i, and birefringence Δn_i as a function of distance from the spinneret were carried out on the running spinning line. The tempera-

Table II Conditions of the High-Speed Melt Spinning of Nylon-66[a]

D (x = 0) cm	T (x = 0) °C	V_L (m/min)	W (g/min)	V_y (cm/min)	T_s (°C)
0.0635	275	3200 4000 6300 6600	2.5	517.040	30

[a] V_y is the velocity of transverse cooling air.

ture profiles were measured with a Barnes infrared (IR) microscope using a noncontact, null balance technique described elsewhere.[10] The diameter and birefringence profiles were measured using an Olympus polarizing microscope mounted at the appropriate position and angle to the running spinning line.[10]

Calculation of the Velocity and dV/dX Profiles

According to eq. 1, the calculated correlation for the velocity and deformation gradient dV/dX is

$$V_i = \frac{4 \times G}{\pi D_i^2 \rho_i} \tag{15}$$

$$\left(\frac{dV}{dX}\right)_i \approx \frac{V_i - V_{i-1}}{X_i - X_{i-1}} \tag{16}$$

where ρ_i is determined by the temperature T_i and crystallization index θ_{i-1}, as shown in the form of eq. 11.

Calculation of the Crystalline Index θ_i and $(d\theta/dX)_i$

From eq. 3, the calculated relationships are

$$\left(\frac{d\theta}{dX}\right)_i \approx \frac{C_p}{\Delta H}\left(\left(\frac{dT}{dX}\right)_i - \frac{\pi h_i D_i (T_s - T_i)}{C_{op} G}\right) \tag{17}$$

$$\theta_i = \left(\frac{d\theta}{dX}\right)_i + \theta_{i-1} \qquad \theta_0 = 0 \tag{18}$$

where

$$\left(\frac{dT}{dX}\right)_i \approx \frac{T_i - T_{i-1}}{X_i - X_{i-1}} \tag{19}$$

and h_i is calculated with eq. 6.

The on-line measurement of temperature and diameter is available, so in this paper we apply these values to the determination of the crystallization gradient and crystalline index.

Calculations of the Amorphous Birefringence $(\Delta n_a)_i$ and $(f_a)_i$

According to eqs. 13 and 14, $(\Delta n_a)_i$ and $(f_a)_i$ are calculated by eqs. 19 and 20, respectively:

$$(\Delta n_a)_i = \frac{\Delta n_i - \theta_i \Delta_c^0 f_c}{1 - \theta_i} \tag{19}$$

$$(f_a)_i = \frac{(\Delta n_a)_i}{\Delta_a^0} \tag{20}$$

Calculation of the Elongational Stress σ_i

The elongational stress was calculated with eq. 21:

$$\sigma_i = \eta_i \times \left(\frac{dV}{dX}\right)_i \tag{21}$$

where η_i is calculated by using the eq. 7.

RESULTS AND DISCUSSION

There still remains a question of how to describe the mechanism of orientation and crystallization. Application of the kinematics of melt spinning, some on-line experimental data, and some literature values of physical properties of Nylon-66 leads to a set of working relationships for calculating other profiles (including the amorphous birefringence, the rate constant of crystallization, etc.) along the spinning line. Using the results of the calculation, we can predict the main factors that affect the structural development at various

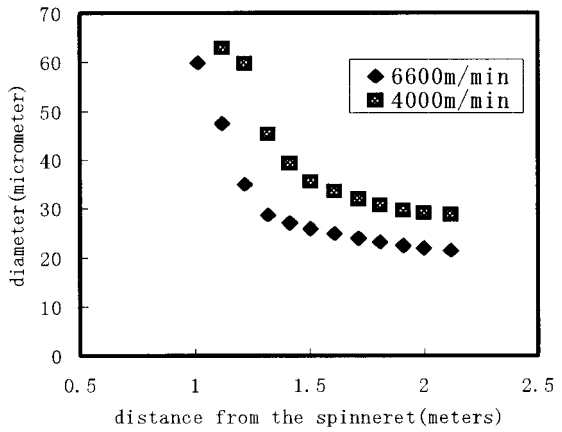

Figure 1 Experimental diameter profiles for Nylon-66 with a mass throughput of 2.5 g/min.

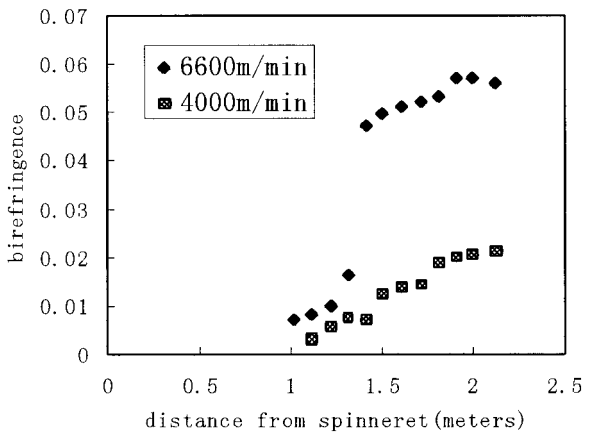

Figure 2 Experimental birefringence profiles for Nylon-66 with a mass throughput of 2.5 g/min.

spinning speeds and discuss the mechanism of orientation and crystallization for high-speed melt spinning of Nylon-66.

On-Line Experimental Results for Nylon-66

The experimental diameter profiles are presented in Figure 1. As in the case of the velocity profiles, at low speed, the diameter draws down smoothly to its final value at the take-up device that would be expected from continuity. At high speed, the diameter draws down more rapidly and to a plateau, where the diameter decreases only slightly thereafter. This result is a consequence of the orientation-induced crystallization within the spinning line. The position where the diameter approaches the plateau is also the point where the birefringence achieves the plateau region (see Figure 2).

The on-line experimental birefringence profiles are shown in Figure 2. At low speed, there is a gradual increase in the birefringence. At high speed, the birefringence starts out increasing slowly, but then rises abruptly at positions corresponding to the onset of rapid crystallization; that is, orientation-induced crystallization occurs.

The on-line experimental temperature profiles are shown in Figure 3. Unlike that of PET, these profiles indicate little variation with regard to spinning speed, and the temperature plateau that results from the latent heat that is released during crystallization is not obvious. This result is because the higher temperature provide a greater ΔT between the filament and its surroundings, which allows the heat of crystallization to be transferred to the surroundings much more efficiently, negating the appearance of a protracted temperature plateau.

Mechanism of Orientation

It seems beyond any doubt that the factor that makes high-speed spinning different from other fiber formation processes is the high tensile stress acting on the polymer melt that is subject to rapid deformation and quenching. The stress acting on polymer chains induces deformation of polymer coils and orientation of chain segments, which in turn contributes to the thermodynamic properties of the polymer, the kinetics and thermodynamics of crystallization, and other structural effects. Molecular orientation controls the modulus, tenacity, and shrinkage of fibers. Therefore, the

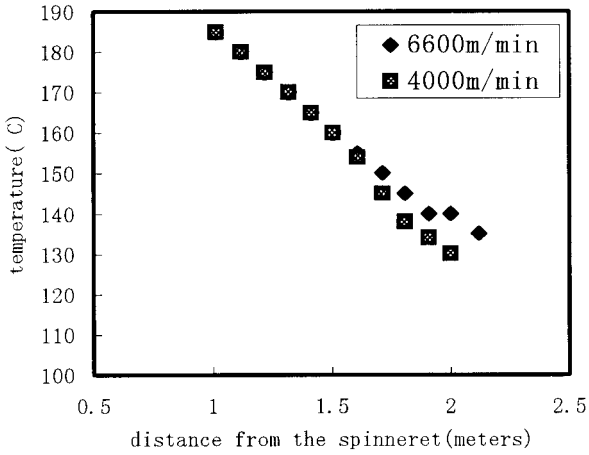

Figure 3 Experimental temperature profiles for Nylon-66 with a mass throughput of 2.5 g/min.

Table III Mathematical Model of Birefringence[a]

Serial Number	Mathematical Model	Remarks
1	$\Delta n \approx C_{op}\sigma_{in} = C_{op}\rho V \Delta V$	$\Delta V = V - V_0$
2	$\Delta n = C_{op}\sigma \approx C_{op}E(\varepsilon + \tau\dot{\varepsilon})$	$\varepsilon = V/V_0$, $\dot{\varepsilon} = dV/dX$, $\tau = \eta/E$
3	$\frac{d\Delta n}{dX} = \frac{C_{op}E}{V}\frac{dV}{dX} - \frac{\Delta n}{V\tau}$	$\tau = \eta/E$
4	$\Delta n = \Delta n_\infty\left\{1 - \exp\left(-\frac{A\sigma}{T+273}\right)\right\}$	A is a constant
5	$\Delta n = \Delta n_\infty\left\{1 - \exp\left(-\frac{A\sigma_{in}}{T+273}\right)\right\}$	$\sigma_{in} = \rho V \Delta V$
6	$\Delta n = \Delta n_\infty\left\{1 - \exp\left(-\frac{A\sigma'}{T+273}\right)\right\}$	$\sigma' = E(\varepsilon + \tau\dot{\varepsilon})$

[a] E is Modulus.

relation between tensile stress and the resulting molecular orientation is crucial for high-speed spinning. Most authors consider constant stress-optical coefficients, which are justified for small stresses and small deformations of idealized polymer chains with Gaussian conformation statistics. Exceptions are provided by the numerical simulation of Katayama and Yoon,[8] who assume a model nonlinear relation between molecular orientation and stress, and by Ziabicki and Jarecki,[7] who propose a nonlinear and non-Gaussian theory of molecular orientation in the entire range of stresses. According to the latter theory, deviations from the linear, "Gaussian" behavior appears at a tensile stress of the order 5×10^7 dyne/cm^2, which is easily attained or exceeded in high-speed spinning. Hamana[7] gives a relation between stress and birefringence as $\Delta n = 7.8 \times 10^{-10}\sigma$ (for PET). This relation is valid only for small stress value. According to the theory of rubber elasticity,[7] Δn is related to $\sigma/(T + 273)$. The mathematical model of the birefringence used herein is shown in Table III.

The experimental birefringence as a function of $\sigma' = E(\varepsilon + \tau\dot{\varepsilon})$ at various spinning speeds is plotted in Figure 4. At the lower take-up speeds, the birefringence increases linearly with the increase of $\sigma' = E(\varepsilon + \tau\dot{\varepsilon})$. At the higher speeds, the birefringence starts out increasing linearly, but then rises abruptly, at positions corresponding to the onset of crystallization, to a new stage in which the birefringence also increases slowly and linearly with the stress.

The results in Figure 4 also indicate that the crystallization rate is greatly enhanced by orientation of the molecules prior to the crystallization process taking place. The driving force for molecular orientation within the spinning line is the stress. At higher take-up speeds, there are two stages in the spinning line; one is a low orientation stage, the other is a rapid orientation increase stage due to the rapid crystallizing. Only in the latter stage is the birefringence deeply affected by the crystallization and does orientation-induced crystallization occur.

Plots of $\ln N = \ln[1 - (\Delta n/\Delta n_\infty)]$ as a function of $Q = \sigma/(T + 273)$, where $\sigma = E(\varepsilon + \tau\varepsilon)$, Δn is the experimental birefringence, and $\Delta n_\infty = 0.2$

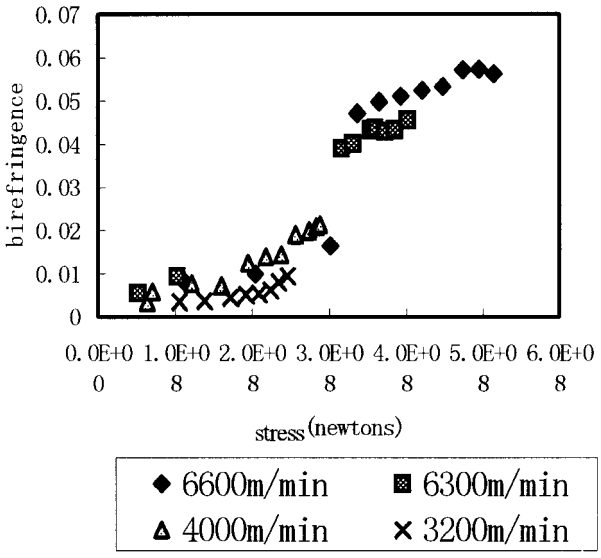

Figure 4 Experimental birefringence as a function of force at various take-up speeds.

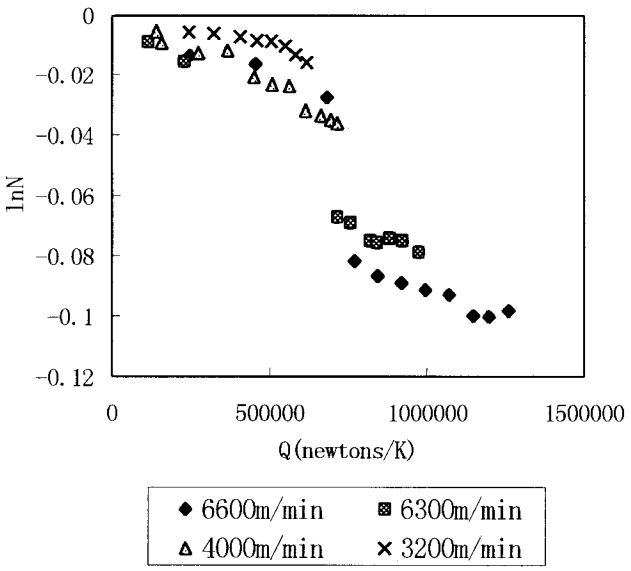

Figure 5 The relationship between $\ln[1 - (\Delta n/\Delta n_\infty)]$ and $\sigma/(T + 273)$.

are shown in Figure 5. At the lower speeds, the decrease in $\ln(1 - \Delta n/\Delta n_\infty)$ with the increase in $\sigma/(T + 273)$ is linear. At the higher speeds, there two stages along the spinning line. One is a low orientation increase stage, the other is a rapid orientation increase stage due to the rapid crystallization. Only in the later stage is the birefringence deeply affected by the crystallization and does orientation-induced crystallization occur.

Figures 4 and 5 are developed from model No. 2 and model No. 6, respectively, based on the rubber-elastic mechanism. The deformation process in the high-speed melt spinning of Nylon-66 has proved to consist of two regions along the spinning line: a Newtonian flow region and a rubber-like deformation region. In the latter region, not only does crystallization occur, but a network of molecules connecting seed crystals may also develop.[18] As the take-up speed is raised, the degree of crystallinity and the crystalline perfection strongly increase, and molecules in the fiber become well oriented and constrained between crystals.

CONCLUSIONS

A new way of applying on-line experimental data and some basic theory to study the mechanism of orientation of a high-speed melt spinning process was described and used to calculate the profiles of Nylon-66 along the spinning line. The relationship that described the birefringence in the model is a combination of the stress optical law and a rubber-elastic element. The results show that the deformation process in the high-speed melt spinning of Nylon-66 consists of two regions along the spinning line: a Newtonian flow region and a rubber-like deformation region. In the latter region, not only does crystallization occur, but a network of molecules connecting seed crystals may also develop.

REFERENCES

1. Ziabicki, A. Kolloid Z 1961, 175, 14.
2. Kase, S.; Matsuo, T. J Text Mach Soc, Japan 1965, 18, 188.
3. Kase, S.; Matsuo, T. J Appl Polym Sci 1967, 11, 251.
4. Kase, S.; Matsuo, T. J Polym Sci 1965, A3, 2541.
5. Yasuda, H.; Sugiyama, H.; Yanagawa, Y. Sen-I Gakkaishi 1979, 35, 370.
6. Prastaro, A.; Parrini, P. Text Res J 1975, 45, 118.
7. Ziabicki, A. Fundamentals of Fiber Formation; Wiley: New York, 1976.
8. Katayama, K.; Yoon, M.-G. In High Speed Fiber Spinning; Ziabicki, A.; Kawai, H., Eds.; Wiley-Interscience: New York, 1985.
9. Shimizu, J.; Okui, N.; Kikutani, T. In High Speed Fiber Spinning; Ziabicki, A.; Kawai, H., Eds.; Wiley-Interscience: New York, 1985.
10. Zieminski, K.; Spruiell, J. E. J Appl Polym Sci 1988, 35, 2223–2245.
11. Sakiadis, B. C. Am Inst Chem Eng J 1961, 7, 467.
12. Schule, E. C. Enc Polym Sci Technol 1969, 10, 557.
13. Heyman, E. Soc Plast Eng J 1967, Oct., 37.
14. Magill, J. H. Polymer 1961, 2, 221.
15. Cannon, C. G.; Chappel, F. P.; Tidmarsh, J. I. J Text Inst 1963, 54, 210.
16. Wunderlich, B. Polym Eng Sci 1978, 18, 431.
17. Taylor, G. B. J Am Chem Soc 1947, 69, 635.
18. Ziabicki, A.; Kawai, H. High-speed Fiber Spinning; 1985.